

An Oil-Based Model of Inhalation Anesthetic Uptake and Elimination

Patrick J. Loughlin, M.S.,* Watson A. Bowes, M.S.,† Dwayne R. Westenskow, Ph.D.‡

An oil-based model was developed as a physical simulation of inhalation anesthetic uptake and elimination. It provides an alternative to animal models in testing the performance of anesthesia equipment. A 7.5-l water-filled manometer simulates pulmonary mechanics. Nitrogen and carbon dioxide flowing into the manometer simulate oxygen consumption and carbon dioxide production. Oil-filled chambers (180 ml and 900 ml) simulate the uptake and washout of halothane by the vessel-rich and muscle tissue groups. A 17.2-l air-filled chamber simulates uptake by the lung group. Gas circulates through the chambers (3.7, 13.8, and 25 l/min) to simulate the transport of anesthetic to the tissues by the circulatory system. Results show that during induction and washout, the rate of rise in end-tidal halothane fraction simulated by the model parallels that measured in patients. The model's end-tidal fraction changes correctly with changes in cardiac output and alveolar ventilation. The model has been used to test anesthetic controllers and to evaluate gas sensors, and should be useful in teaching principles underlying volatile anesthetic uptake. (Key words: Anesthetics, volatile; pharmacokinetics. Pharmacokinetics, models: oil-based.)

PHYSICAL MODELS of gas exchange (\dot{V}_{O_2} and \dot{V}_{CO_2}) and pulmonary mechanics are used extensively to test ventilators and ICU monitors.¹⁻⁵ Equivalent physical models of anesthetic uptake, that allow one to test anesthetic equipment, are not available. To date, volatile anesthetic uptake has been modeled using electrical analogues and computers.⁶⁻¹⁴ Although these models help conceptualize the dynamics of anesthetic uptake, they cannot be used with actual breathing circuits, and they cannot be used to test anesthetic delivery devices and gas monitors. We describe an oil-based model of anesthetic uptake and elimination which fills this need. The model is validated by comparing the rate of rise for the model's end-tidal halothane concentration with the rate of rise measured in earlier patient studies and computer simulation.

Methods

The model is shown in figure 1. Pulmonary mechanics, functional residual capacity (FRC), and anatomical dead space are modeled by a water-filled manometer.⁵ The FRC is the air space above the water as labeled in figure 1. The anatomic deadspace is the volume of the tube connecting the FRC to the endotracheal tube. When a tidal volume is added to the FRC, the water rises in the opposite side of the manometer, creating end-inspiratory pressure. A model with the dimensions described in the legend to figure 1 has a compliance ($\Delta V/\Delta P$) of 0.1 l/cm H₂O. A resistance placed on the inlet to the FRC will simulate airway resistance (*i.e.*, 10 cm H₂O · l⁻¹ · s⁻¹). The pressure-volume curve of the model closely matches that seen in patients whose lungs are mechanically ventilated.⁵ Gas exchange (\dot{V}_{CO_2} and \dot{V}_{O_2}) can be modeled by bubbling CO₂ and N₂ into the FRC. \dot{V}_{O_2} is calculated from the N₂ flow rate (\dot{V}_{N_2}) by the relationship:

$$\dot{V}_{O_2} = \dot{V}_{N_2} F_{IO_2} / (1 - F_{IO_2}).^{1-4}$$

Three physical compartments model volatile anesthetic uptake by body tissues.⁶⁻⁸ These compartments represent, and will be referred to as, the lung and blood group (LG), the vessel-rich group (VRG), and the muscle group (MG). The VRG and MG are modeled by olive oil-filled chambers in parallel with the lung compartment. Tissue/oil partition coefficients ($\lambda_{t/oil}$), table 1, are used to calculate equivalent oil volumes (V_{oil}) for the VRG and MG such that, at equilibrium, the amount of anesthetic in the saturated oil equals the amount in the saturated tissue:

$$V_{oil} = V_t \cdot \lambda_{t/oil} \quad (1)$$

(V_t = volume of tissue). The LG is a gas filled mixing chamber. Its equivalent volume (V_{gas}) is calculated using the tissue/gas partition coefficients ($\lambda_{t/g}$) for lung tissue and blood:

$$V_{gas} = V_t \cdot \lambda_{t/g}. \quad (2)$$

The model does not include a fat group or a vessel-poor group. These two groups do not significantly contribute to uptake during the first hour of anesthetic induction,⁶ and to model halothane uptake by these groups would require approximately 12 l of oil.

* Graduate Student.

† Medical Student.

‡ Professor.

Received from the Department of Anesthesiology, The University of Utah, Salt Lake City, Utah. Accepted for publication March 21, 1989. Supported in part by Drägerwerk, West Germany. Presented in part at the Annual Meeting of American Society of Anesthesiologists, October 1988, San Francisco, California; and at the IEEE Engineering in Medicine and Biology Society 10th Annual International Conference, November 1988, New Orleans, Louisiana.

Address reprint requests to Dr. Westenskow: Department of Anesthesiology, The University of Utah, 50 North Medical Drive, Salt Lake City, Utah 84132.

To simulate the rapid gas exchange which takes place between alveolar gas, pulmonary blood, and lung tissue, gas is pumped from the FRC through the gas mixing chamber (LG) at 25 l/min, the maximum rate provided by a small blower (Mini-Spiral,[®] EG&G Rotron, New York). At this flow rate, the "time constant" for the 17.2 l LG is approximately 40 s.

To simulate the blood flow which perfuses the VRG and MG, gas is pumped from the FRC, through the two oil chambers using two Mini-Spiral blowers. The flow of gas through the oil chambers (\dot{V}_g) was adjusted to simulate the blood flow to each group (\dot{Q}_b):

$$\dot{V}_g = 1.6 \cdot \dot{Q}_b \cdot \lambda_{b/g} \quad (3)$$

where $\lambda_{b/g}$ is the blood/gas partition coefficient. Tissue group blood flows (\dot{Q}_b) were determined according to Eger¹⁶ (table 1). The constant 1.6 accounts for an apparent oil/gas mixing inefficiency. In the oil model, the diffusion of anesthetic vapor from the circulating gas to the oil is not as efficient as is the diffusion from capillary blood to tissue in the human body. The factor 1.6 was found by adjusting the cardiac output (CO) in the Zwart model¹⁰ until the computer simulated end-tidal concentrations matched the oil-model concentrations. The oil model was calibrated against the Zwart model because of the limited quantity of patient data documenting the effects of CO and \dot{V}_A on end-tidal anesthetic fraction. These effects can be simulated by the Zwart model.¹⁰

A factor is also needed so that the oil model's rate of rise in $F_{ET\text{hal}}$ changed with V_A during induction, as predicted by the Zwart model. The oil model's end-tidal anesthetic concentration changes correctly with changes in \dot{V}_A when the following relationship is used:

$$\dot{V}_A = 0.5 \dot{V}_{A\text{oil}} + 2.1 \quad (4)$$

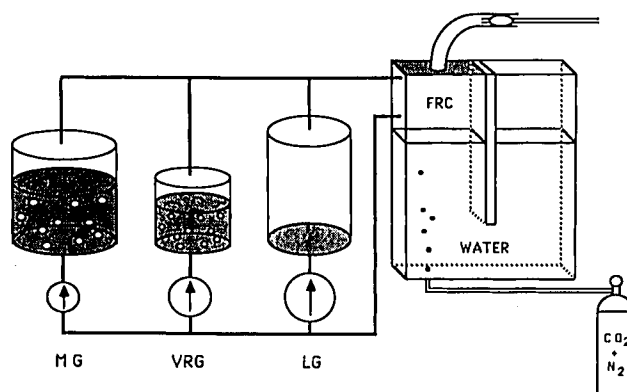


FIG. 1. A physical model of anesthetic uptake, gas exchange, and pulmonary mechanics. The lung for a 70 kg adult is modeled using a 14 cm × 14 cm × 38 cm water manometer. A 2 l FRC is shown on the left side. A series dead space (100 ml) is shown at the top, intubated with a cuffed endotracheal tube. The lung tissue group (LG) is modeled for halothane with a 17.2 l air-filled mixing chamber and a gas flow of 25 l/min. The muscle group (MG) and vessel rich group (VRG) are modeled using olive oil, with volumes of 900 ml and 180 ml for halothane, and flows of 3.7 l/min and 13.8 l/min, respectively (calculated using table 1 and equations 1 and 3). CO₂ and N₂ bubbling into the FRC simulate $\dot{V}CO_2$ and $\dot{V}O_2$.

where $\dot{V}_{A\text{oil}}$ is the ventilation rate of the oil model and \dot{V}_A is the simulated patients' alveolar ventilation (l/min). The Zwart computer simulation was again used to find this relationship.

TEST METHODS

The end-tidal halothane fraction ($F_{ET\text{hal}}$) for the oil model was measured during induction and washout by connecting the model to an anesthesia circuit (Drägerwerk, Lubeck, West Germany) and ventilator (Ventime-

TABLE 1. Constants used to Simulate Halothane Uptake

Tissue Group	V_t (l)	\dot{Q}_b (l/min)	HAL		ENF		ISO		
			$\lambda_{t/g}$	$\lambda_{t/oil}$	$\lambda_{t/g}$	$\lambda_{t/oil}$	$\lambda_{t/g}$	$\lambda_{t/oil}$	
LG	FRC	2.0	1.0		1.0		1.0		
	Blood	5.4	2.3		1.9		1.5		
	Lung Tissue	0.6	4.6		3.8		3.0		
VRG	Brain	1.5	6.15	.027	3.03	.031	3.65	.039	
	Heart	0.3	6.72	.030	3.05	.031	5.58	.059	
	Kidney	0.3	4.02	.018	2.23	.023	1.98	.021	
	Liver	3.9	7.24	.032	3.80	.039	3.50	.037	
MG	Muscle	30.1	1.0	6.72	.030	3.05	.031	5.58	.059

Volumes, blood flows, and partition coefficients as used in the oil model to simulate halothane uptake for a 70 kg adult. Tissue volumes (V_t) are taken from Mapleson.⁸ The blood flow (\dot{Q}_b) to each tissue group assumes a cardiac output of 5 l/min.¹⁶ Tissue/gas ($\lambda_{t/g}$) and olive oil/gas ($\lambda_{t/oil}$) partition coefficients are taken from Lowe.²³ Tissue/oil partition coefficients ($\lambda_{t/oil}$) are calculated by dividing the tissue/

gas partition coefficients by the olive oil/gas partition coefficients. Tissue/oil partition coefficients are not given for the LG because this group is modeled using air. Heart muscle is assumed to have the same partition coefficient as skeletal muscle. Brain/gas partition coefficients are for whole brain (ENF, ISO) or for an average of white and grey matter (HAL).

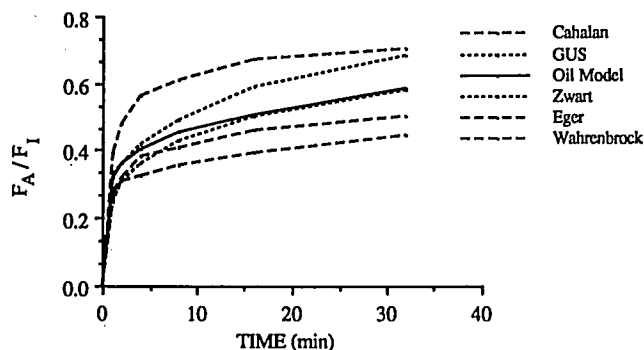


FIG. 2. The alveolar halothane fraction divided by the inspired halothane fraction (F_A/F_I) during induction for the oil model (solid line), for the two computer simulations GUS and Zwart,¹⁰ (short-dashed lines) and for the patient studies of Eger,¹⁶ Cahalan,¹⁵ and Wahrenbrock¹⁷ (long-dashed lines). The curve for the oil model is the mean of three measurements with $\dot{V}_A = 5$ l/min and $\dot{V}_A = 4.2$ l/min.

ter, Narco Medical, PA). Halothane was delivered in 100% oxygen (5 l/min) through a Drager vaporizer. The inspired halothane concentration (F_{Ihal}) was held constant at 1.0 vol% during induction. The F_{Ihal} and F_{EThal} were measured using an IRINA infrared agent analyzer (Dragerwerk) which was placed between the circuit y-piece and the endotracheal tube. The signal from the IRINA was filtered (low-pass corner frequency = 0.7 Hz) and sampled (2 samples/s) by a MINC-11/23 computer (Digital Equipment Corporation, MA). F_{Ihal} and F_{EThal} were determined every 10 s by selecting the maximum and minimum values from a 10 s data buffer.

Before connecting the oil model to the breathing circuit, the vaporizer was set at 1.0 vol% halothane and gas within the circuit was allowed to equilibrate for 20 min. The breathing circuit was then connected to the oil model, and F_{Ihal} and F_{EThal} were recorded for 32 min. After 32 min, the vaporizer was turned off and F_{Ihal} and F_{EThal} were recorded during 32 min of washout. This sequence was repeated three times with a cardiac output (CO) of 5 l/min and alveolar ventilation (\dot{V}_A) of 4.2 l/min. Three simulations were also made with CO = 2.5 l/min and three with CO = 7.5 l/min. F_{EThal} was also measured during three simulations with CO = 5 l/min and $\dot{V}_A = 2.1$ l/min, and three with CO = 5 l/min and $\dot{V}_A = 8.4$ l/min. F_{ETenf} (enflurane) was measured using an F_{Ienf} of 1.0 vol% and F_{ETiso} (isoflurane) was measured using an F_{Iiso} of 1.0 vol% isoflurane with CO = 5 l/min and $\dot{V}_A = 4.2$ l/min.

The data obtained from the oil model were filtered (digital low-pass, 4th-order, zero-phase Butterworth filter, corner frequency = 0.01 Hz), and plotted along with

published patient data¹⁵⁻¹⁷ and computer simulation results from the Zwart¹⁰ and GUS models. § The end-tidal concentrations were assumed to equal alveolar concentrations and the measurements expressed as an alveolar to inspired fraction F_A/F_I .

The Zwart computer model¹⁰ simulates blood flow and halothane transport to nine tissue compartments. Venous blood is collected in the vena cava and goes to the lung and/or through a lung shunt to the arterial compartment. This model was modified so that CO remained constant during uptake and washout (as it did for the oil model). The GUS computer model simulates anesthetic uptake and distribution using a numerical model with 27 gas, blood, and tissue compartments. Transport of anesthetic agents among the compartments occurs *via* convection of gas and blood during discrete iterations of the simulation.

Results

Figure 2 compares the halothane alveolar to inspired ratio (F_A/F_I) for the oil model with patient data and computer simulation. The oil model F_A/F_I most closely matches the Zwart computer simulation (as expected), and falls between the patient curves. The standard deviation between three repeated oil model simulations of F_A/F_I averaged 2.7% of reading.

Changes in F_A/F_I which accompany changes in cardiac output are shown in figure 3. The upper curve is for CO = 2.5 l/min, the lower curve for CO = 7.5 l/min.

Figure 4 shows the changes in F_A/F_I which accompany changes in \dot{V}_A . The upper curve is for $\dot{V}_A = 8.4$ l/min, the lower for $\dot{V}_A = 2.1$ l/min.

Figure 5 shows the oil model simulation of halothane, enflurane, and isoflurane F_A/F_I . The relative rates of rise of F_A/F_I are comparable with those seen in patients and in computer simulations.

Discussion

Models help us understand physiology and are useful in teaching and training. Using our physical oil model, training can be conducted in a mock clinical setting where anesthetic uptake and elimination can be simulated and the effects of ventilation and cardiac output demonstrated, using actual anesthesia machines, patient breathing circuits, and gas monitoring devices. The model is also valuable as a research tool, in testing and evaluating new devices. Vaporizers, ventilators, and anesthetic agent analyzers can be tested and evaluated under simulated clinical situations. The noise generated by the model adds realism to these evaluations.

A water manometer was first described by J. Brunner⁵ for the simulation of pulmonary mechanics, intrapulmonary gas mixing, and $\dot{V}CO_2$. Realistic values for compli-

§ Gas Uptake Simulation (GUS). Imed Ed Inc., 2701 E. Camelback Road, Suite 205, Phoenix, Arizona 85016.

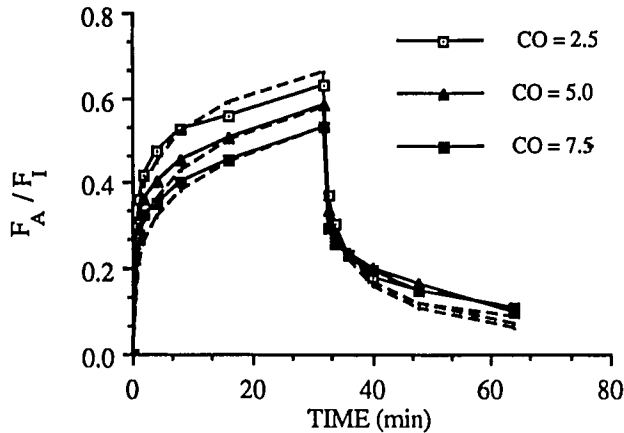


FIG. 3. The effect of cardiac output on halothane F_A/F_I . The solid lines show the results from the oil model simulation, the dashed lines show computer simulation.¹⁰ $\dot{V}_A = 4.2$ l/min and CO = 2.5, 5.0 and 7.5 l/min. Each oil model curve is the average of three measurements. For simplicity, the results during washout (32–64 min) are expressed as F_A/F_I where $F_I = 1.0$, even though $F_I = 0$ during washout.

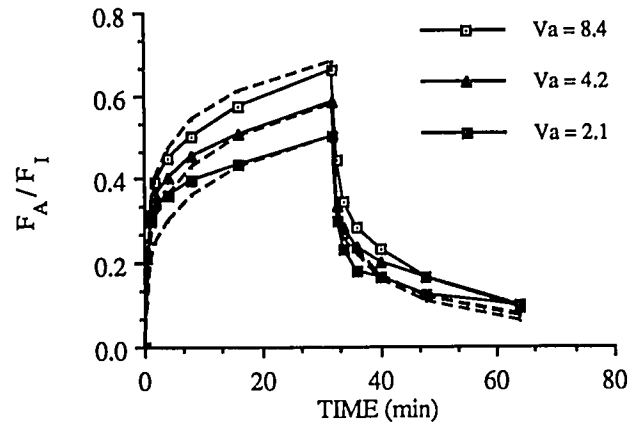


FIG. 4. The effect of alveolar ventilation on halothane F_A/F_I . Results from the oil model simulation shown with solid lines, dashed lines show the computer simulation.¹⁰ CO = 5.0 l/min and $\dot{V}_A = 2.1, 4.2,$ and 8.4 l/min. Each oil model curve is the average of three measurements.

ance, resistance, lung volume, and dead space are achieved by selecting appropriate dimensions for the two water-filled chambers and for the gas inlet tube (trachea). Spontaneous ventilation may be simulated by connecting a mechanical ventilator to the right chamber in figure 1 and by using inverse I:E ratios. CO₂ bubbling through the water simulates CO₂ production; the expired CO₂ waveform is very realistic. Nitrogen dilution is a standard technique for simulating oxygen consumption; it is a standard used in assessing the accuracy of oxygen consumption monitors.^{1-4,18,19} Unfortunately, this method cannot be used to simulate $\dot{V}O_2$ during closed circuit anesthesia; nitrogen dilution causes the expired tidal volume to be larger than the inspired tidal volume. An alcohol, propane, or hydrogen flame burning in the FRC chamber provides a more realistic simulation of $\dot{V}O_2$ and $\dot{V}CO_2$.^{18,20}

We added anesthetic uptake to the water manometer model by adding oil chambers. The oil model's simulation of the rate of rise of end-tidal halothane concentration during induction closely matches the Zwart and GUS computer simulations and falls within the range of patient data. The match with the Zwart model is expected, as the oil model was calibrated against the Zwart model. We could have calibrated our model to match one of the patient curves shown in figure 2. However, the published patient data¹⁵⁻¹⁷ do not report the CO and \dot{V}_A under which the patient data were obtained; therefore, we chose to calibrate the oil model to the Zwart model. The result was an F_A/F_I for the oil model, which is lower than that reported in the Cahalan¹⁵ patient study and higher than that reported in the Eger¹⁶ and Wahrenbrock¹⁷ patient studies.

The oil model simulation of $F_{ET,hal}$ is affected by \dot{V}_A and CO, but to a lesser extent than expected.^{6,21} Mixing and diffusion are obviously not as efficient in the oil model as they are in the natural lung. The alveolar/blood and blood/tissue surface areas are much larger in the body than are the oil/gas surface areas in the oil model. Factors 1.6 in equation 3 and 0.5 in equation 4 were found to compensate for these inefficiencies. More work is needed to verify that these factors are linear and apply over larger ranges of CO and \dot{V}_A for each anesthetic agent. A mixing fan in the FRC,⁵ and smaller bubbles in the oil chambers, might change the value of the constants or make them unnecessary.

\dot{V}_A and CO had little effect on the rate of halothane washout for either the oil model or the computer simulation (figs. 3,4). The small effect may be due to the relatively short duration of anesthetic exposure and the small

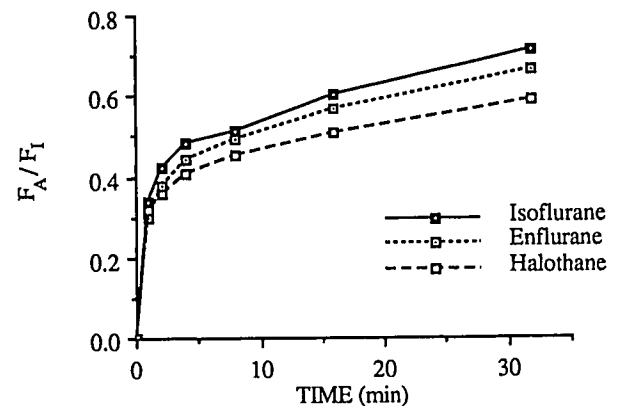


FIG. 5. F_A/F_I for isoflurane, enflurane, and halothane as simulated by the oil model. CO = 5 l/min and $\dot{V}_A = 4.2$ l/min. Each curve is the average of three measurements.

venous-to-alveolar partial pressure gradient (especially for short duration anesthesia).^{6,21,22} During washout, $F_{ET}hal$ for the oil model was somewhat higher than $F_{ET}hal$ predicted by the Zwart computer simulation. The release of halothane from the breathing circuit components may have caused this difference (the computer simulations did not model the breathing circuit and its effects on washout).

Our oil model does not correctly simulate the second gas effect. The oil volumes and gas flows given by equations 1–3 are agent-specific: they depend on the $\lambda_{t/g}$ and $\lambda_{b/g}$ of each agent. Further, our model does not simulate uptake by the fat tissue or the vessel-poor tissue groups; therefore, it does not properly simulate anesthetic uptake after the first 1–2 h of induction. Our model also neglects the effects of metabolism of anesthetic agent; metabolism accounts for a significant fraction of the halothane elimination.¹⁵ Finally, changes in CO were proportionally distributed to each tissue group in our model. This is an oversimplification of the nonlinear cardiovascular dynamics and nonuniform distribution of CO which occurs in patients. Although changes in \dot{V}_A and CO in the oil model produce changes in F_A/F_I which are consistent with the Zwart model, they may not match reality. Pharmacokinetic models rely on our limited knowledge of human physiology. Similarly, a model as simple as ours cannot possibly simulate the complex interactions between the brain anesthetic partial pressure, CO and \dot{V}_A .

We make extensive use of the model in our research laboratory to test and evaluate new gas monitoring equipment. Control systems being developed to regulate the end-tidal concentration of anesthetic are tested with the model using actual anesthetic delivery devices and breathing systems. The model has bridged the gap between computer simulations and clinical reality, and in doing so has, in our laboratory, reduced the number of animal and clinical experiments needed to evaluate new equipment.

The authors wish to thank Robert G. Loeb, M.D., and Josef X. Brunner, Ph.D., for their suggestions and contributions. They also wish to thank Lue-Ellen Merchant for her assistance in the preparation of this article.

References

1. Kappagoda CT, Linden RJ: A critical assessment of an open circuit technique for measuring oxygen consumption. *Cardiovasc Res* 6:589, 1972
2. Damask MC, Weissman C, Askanazi J, Hyman AI, Rosenbaum SH, Kinney JM: A systematic method for validation of gas exchange measurements. *ANESTHESIOLOGY* 57:213–218, 1982
3. Lister G Jr., Hoffman JIE, Rudolph AM: Measurement of oxygen consumption: Assessing the accuracy of a method. *J Appl Physiol* 43:916–917, 1977
4. Fixler DE, Carrell T, Browne R, Willis K, and Miller WW: Oxygen consumption in infants and children during cardiac catheterization. *Circulation* 50:788–794, 1974
5. Brunner JX, Wolff G: *Pulmonary Function Indices in Critical Care Patients*. New York, Springer-Verlag, 1988, pp 59–61
6. Eger EI II: *Anesthetic Uptake and Action*. Baltimore, Williams and Wilkins, 1974, pp 88–89, 105
7. Mapleson WW: An electric analogue for uptake and exchange of inert gases and other agents. *J Appl Physiol* 18:197–204, 1963
8. Mapleson WW: Inert gas exchange theory using an electric analogue. *J Appl Physiol* 19:1193–1199, 1964
9. Ashman MN, Blesser WB, Epstein RM: A nonlinear model for the uptake and distribution of halothane in man. *ANESTHESIOLOGY* 33:419–429, 1970
10. Zwart A, Smith NT, Beneken JEW: Multiple model approach to uptake and distribution of halothane: The use of an analog computer. *Comput Biomed Res* 5:228–238, 1972
11. Smith NT, Zwart A, Beneken JEW: Interaction between the circulatory effects and the uptake and distribution of halothane: Use of a multiple model. *ANESTHESIOLOGY* 37:47–57, 1972
12. Mapleson WW: Circulation-time models of the uptake of inhaled anaesthetics and data for quantifying them. *Br J Anaesth* 45:319–333, 1973
13. Fukui Y, and Smith NT: Interactions among ventilation, the circulation, and the uptake and distribution of halothane—Use of a hybrid computer multiple model: I. The basic model. *ANESTHESIOLOGY* 54:107–118, 1981
14. Zbinden AM, Frei F, Westenskow DR, Thomson DA: Control of end-tidal halothane concentration. Part B: Verification in dogs. *Br J Anaesth* 58:563–571, 1986
15. Cahalan MK, Johnson BH, Eger EI II: Relationship of concentrations of halothane and enflurane to their metabolism and elimination in man. *ANESTHESIOLOGY* 54:3–8, 1981
16. Eger EI II: Uptake and distribution of inhaled anesthetics, *Anesthesia*. Edited by Miller RD. New York, Churchill Livingstone, 1986, pp 309–331
17. Wahrenbrock EA, Eger EI II, Laravuso RB: Anesthetic uptake of mice and men (and whales). *ANESTHESIOLOGY* 40:19–23, 1974
18. Merilainen PT: Metabolic monitor. *Int J Clin Monit Comput* 4:167–177, 1987
19. Westenskow DR, Cutler CA, Wallace WD: Instrumentation for monitoring gas exchange and metabolic rate in critically ill patients. *Crit Care Med* 3:183–187, 1982
20. Stenqvist O, Sonander H, Lofstrom B, Nilsson K: An oxygen-consuming model lung for evaluation of anaesthetic circuits. *Acta Anaesthesiol Scand* 26:322–326, 1982
21. Yamamura H, Wakasugi B, Okuma Y, Maki K: The effects of ventilation on the absorption and elimination of inhalation anesthetics. *Anaesthesia* 18:427–437, 1963
22. Stoelting RK, and Eger EI II: The effects of ventilation and anesthetic solubility on recovery from anesthesia: An *in vivo* and analog analysis before and after equilibration. *ANESTHESIOLOGY* 30:290–296, 1969
23. Lowe HJ, Ernst EA: *Use of closed circuit, The Quantitative Practice of Anesthesia*. Baltimore, Williams and Wilkins, 1980, pp 57, 214–215